

Q-Balancing in Periodic Leaky-Wave Antennas to mitigate Broadside Radiation Issues

Simon Otto, Amar Al-Bassam, Zhichao Chen, Andreas Rennings, Klaus Solbach, and Christophe Caloz

Department HFT & ATE, University of Duisburg-Essen, Bismarckstr. 81, 47057 Duisburg, Germany
Ecole Polytechnique de Montreal, 2500, ch. de Polytechnique, H3T 1J4, Montreal, Quebec, Canada

Abstract—This paper illustrates and applies the recently established Q-balancing condition in frequency-scanning periodic leaky-wave antennas (LWAs) for achieving a frequency independent leakage factor and input impedance. The unit cells of such LWAs can be modeled by an equivalent two-port network comprising two independent circuit elements, a series resonator and a shunt resonator, which are characterized by their resonance frequencies (f_{se}, f_{sh}) and quality factors (Q_{se}, Q_{sh}), where the quality factors correspond to the reactive energies stored over the radiated and dissipated powers in each respective resonator. The Q-balancing condition consists in achieving equal quality factors for the series and the shunt resonator: $Q_{se} = Q_{sh}$. Here, we propose two general concepts—the resistive loading concept—and—the asymmetry concept—to design LWAs based on the Q-balancing criteria. Furthermore, we apply the aforementioned concepts to the specific example of a series-fed patch array (SFPA) LWA to obtain a frequency independent input impedance and hence a constant gain for the LWA radiation through broadside.

Index Terms—Leaky-wave antenna, broadside radiation, Q-balancing, Bloch impedance, series-fed patch array (SFPA).

I. INTRODUCTION

A one-dimensional periodic leaky-wave antenna (LWA) is formed by periodic repetition of antenna unit cell elements along the antenna axis [1]. In this type of antenna a traveling-wave is guided along the antenna structure that partially leaks out due to radiation at the periodic discontinuities. While one side of the LWA is excited, the other side is either terminated by a matched load or electrically far away from the excitation side (power is leaked out before reaching the end), so to ensure a reflectionless antenna end. The main beam radiation angle in a LWA is varied by frequency. The frequency controls the wavelength of the guided traveling wave and hence excite the radiating discontinuities with a phase progression at lower frequencies (backward radiation), in-phase at an intermediate broadside frequency (broadside radiation) and with phase lack at higher frequencies (forward radiation).

The broadside radiation is most critical due to a standing wave phenomena and a resulting open-stopband [2]. Recently, there has been a strong focus on broadside radiation, particularly on composite right/left-handed (CRLH) LWAs [3],[4], with an empirically optimized CRLH LWA design presented in [5] to overcome the problems at broadside. Some underlying theory has been reported three years later in [6], where a parameter relation for the CRLH equivalent circuit model

has been derived for achieving a constant leakage factor and Bloch impedance. At the same time a more rigorous approach for a general class of one-dimensional periodic LWAs has been established in [7], where the open-stopband issue has been solved by fulfilling two independent conditions: the *frequency-balancing condition* with $f_{se} = f_{sh}$, which is already well known for closing the band gap [3] and the newly derived *Q-balancing condition* with $Q_{se} = Q_{sh}$ for achieving a frequency invariant leakage factor and Bloch impedance, while the radiation beam is steered through the broadside direction. The Q-balancing condition corresponds to the Heaviside condition in conventional lossy transmission lines to obtain distortionless propagation [8]. In this paper we propose two concepts, the *resistive loading concept* and the *asymmetry concept* for achieving Q-balancing in periodic LWAs to mitigate broadside radiation issues. In some LWAs [7], [9] the series resonator is mainly contributing to radiation as compared to the shunt resonator and has therefore a lower quality factor ($Q_{se} < Q_{sh}$).

Both proposed concepts offer the possibility to tune the shunt quality factor so to effectively match it to the series quality factor. The resistive loading concept simply introduces lumped element resistors to increase the dissipation loss in the shunt resonator and hence lowering Q_{sh} . The asymmetry concept increases the shunt radiation in broadside direction, which is orthogonally polarized with respect to the series radiation contribution. Both concepts can be generally applied to a broad class of periodic LWAs, yet we chose the example of a series-fed patch array (SFPA) LWA to demonstrate them both and to illustrate the Q-balancing for achieving a constant leakage factor and a constant Bloch impedance. This ultimately results in a constant radiation efficiency, gain and beamwidth when the LWA radiation beam is steered through the broadside direction.

II. TWO-PORT UNIT CELL MODELING OF A SERIES-FED PATCH ARRAY (SFPA) ANTENNA

This section briefly reviews the *equivalent transmission line modeling* for periodic LWAs [7] in order to derive the specific Q-balancing condition for the SFPA LWA. Finally, an illustration for Q-balancing is presented, where we compare the propagation constant and the impedance for balanced and unbalanced cases.

A. Equivalent Transmission Line Modeling for Periodic Structures

Fig. 1 shows four different two-port models of a LWA unit cell. While the layout and the circuit in Figs. 1(a) and 1(b) are specific to the SFPA LWA, the model in Figs. 1(c) and 1(d) are general and might be applied to a broad class of one-dimensional LWAs. The equivalent transmission line (TL) model for a periodic LWA in Fig. 1(d) is a simple model for which analytical formulas have been derived in [7], that is capable to model and explain fundamental physics in LWA scanning through broadsided. First, the constitutive LCRG parameters for this TL model will be calculated analytically based on the circuit of the SFPA in Fig. 1(b) and the perturbation approach presented in [7]. Upon the basis of this calculated LCRG parameters, the Q-balancing condition is subsequently derived for the SFPA circuit in Fig. 1(b). Later, in Sec. III the LCRG parameters are directly and accurately obtained through numerical full-wave simulation using the procedures described in [7] and [9].

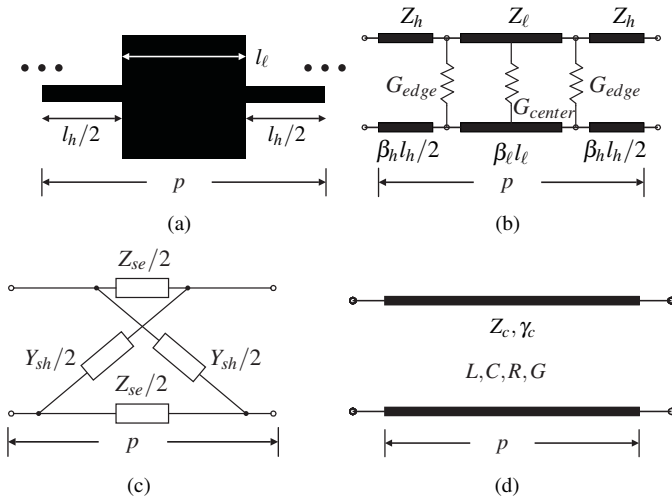


Fig. 1. Two-port modeling of a series-fed patch antenna unit cell with increasing level of abstraction from (a) to (d). (a) microstrip metalization layout for the use in a full-wave simulator. (b) simplified broadband circuit model composed of distributed transmission line sections and concentrated loss elements. (c) lattice model for the separation of series and shunt contributions. (d) equivalent transmission line model with its four constitutive parameters (LCRG) obtained from a linearization and homogenization of the lattice in (c).

Any symmetrical two-port network can be represented by the lattice topology of Fig. 1(c), since so far there are no restrictions imposed on the impedance Z_{se} and the admittance Y_{sh} . For the lattice circuit we recall the exact Bloch properties (index B), the propagation constant and the impedance from [7] with

$$\gamma_B p = \alpha_B p + j\beta_B p = \cosh^{-1} \frac{4 + Z_{se} Y_{sh}}{4 - Z_{se} Y_{sh}} \quad \text{and} \quad Z_B = \sqrt{\frac{Z_{se}}{Y_{sh}}}. \quad (1)$$

In many periodic LWAs these immittances Z_{se} and Y_{sh} follow a series and a shunt resonance behavior with ω_{se} and ω_{sh} as resonance frequencies, respectively. The immittances

might be linearized around their resonance frequencies for obtaining a simple analytical model [7]. Assuming a small frequency deviation $\Delta\omega = \omega - \omega_0$ from $\omega_{se} = \omega_{sh} = \omega_0$, where ω_0 is the broadside radiation frequency, we write $Z_{se} \approx Z_{se,l} = R + j2L\Delta\omega$ and $Y_{sh} \approx Y_{sh,l} = G + j2C\Delta\omega$, so to obtain linear reactance and susceptance in frequency, while the radiation/loss contributions are assumed to be constant. Using a homogenization procedure (propagation constant $|\gamma_B| \rightarrow 0$), we approximate the Bloch propagation constant and the Bloch impedance with the characteristic propagation constant and the characteristic impedance with index c:

$$\gamma_c p = (\alpha_c + j\beta_c) p = \sqrt{Z_{se,l} Y_{sh,l}} \quad \text{and} \quad Z_c = \sqrt{\frac{Z_{se,l}}{Y_{sh,l}}}. \quad (2)$$

B. LCRG Parameters and the Q-Balancing Condition for the SFPA LWA

The SFPA is modeled in Fig. 1(b) by alternating low and high impedance (Z_ℓ, Z_h) ideal transmission line sections with the radiation accounted for by the resistive elements G_{edge} and G_{center} , where G_{edge} models the radiating edges of the microstrip patch (broadside radiation) and G_{center} models the minor lateral radiation to the sides (broadside radiation is canceled due to symmetry). Both resistors include radiation as well as dissipation contributions. We now assume an electrical length of $\beta_h l_h/2 = 90^\circ$ for the high impedance TL sections and an electrical length of $\beta_\ell l_\ell = 180^\circ$ for the low impedance TL section, respectively at the broadside frequency ω_0 . The details of the procedure to derive the LCRG parameter are given in [7] and they are not repeated here. First, we evaluate the reactive contributions for the lattice in Fig. 1(c) by neglecting the losses in Fig. 1(b) with $G_{center} = 0$ and $G_{edge} = 0$. For the immittances of the lattice circuit we find

$$Z_{se} = j2Z_h \frac{(Z_h + Z_\ell) \sin(\pi\omega/\omega_0)}{Z_h - Z_\ell + (Z_h + Z_\ell) \cos(\pi\omega/\omega_0)} \quad (3a)$$

and

$$Y_{sh} = \frac{j2}{Z_h} \frac{(Z_h + Z_\ell) \sin(\pi\omega/\omega_0)}{Z_\ell - Z_h + (Z_h + Z_\ell) \cos(\pi\omega/\omega_0)}. \quad (3b)$$

The derivatives of Z_{se} and Y_{sh} in Eqs. (3) at the broadside frequency ω_0 leads to the LC parameters with

$$L = \frac{\pi}{2\omega_0} Z_h \frac{Z_\ell + Z_h}{Z_\ell} \quad \text{and} \quad C = \frac{\pi}{2\omega_0} \frac{Z_\ell + Z_h}{Z_h^2}. \quad (4)$$

If now the loss elements are introduced and the circuit of Fig. 1(b) is evaluated at ω_0 , we get

$$R = 2Z_h^2 G_{edge} \quad \text{and} \quad G = \frac{Z_\ell^2}{Z_h^2} G_{center}. \quad (5)$$

The quality factors of the two resonance circuits are

$$Q_{se} = \frac{\omega_0 L}{R} \quad \text{and} \quad Q_{sh} = \frac{\omega_0 C}{G}. \quad (6)$$

Finally, applying the Q-balancing condition with $Q_{se} = Q_{sh}$ or $L/C = R/G$, we can explicitly derive a closed-form expression for the resistive elements in the SFPA circuit of Fig. 1(b) with:

$$G_{center} = 2 \frac{Z_h}{Z_\ell} G_{edge}. \quad (7)$$

While G_{edge} is accounting for the dominant patch radiation directed to broadside, G_{center} is modeling minor lateral radiation to the sides, therefore we have $Q_{sh} > Q_{se}$.

An example comparing propagation constant and impedance for different Q-conditions is illustrated in Fig. 2. We choose a set of parameters: $Z_h = 100 \Omega$, $Z_\ell = 25 \Omega$, $G_{edge} = [3.927, 0.196, 3.927] \text{ mS}$ and $G_{center} = [1.571, 31.416, 31.416] \text{ mS}$, where the conductivity lists correspond to the plots in Fig. 2 as follows $G = [(a) \text{ and } (b), (c) \text{ and } (d), (e) \text{ and } (f)]$. In general, both models, Bloch and TL, agree well in the considered frequency range. For the plots in Figs. 2(e) and 2(f), where the Q-balanced condition is depicted, we used Eq. (7) to calculate $G_{center} = 31.416 \text{ mS}$ based on a given $G_{edge} = 3.927 \text{ mS}$. A constant leakage factor and a constant impedance around ω_0 is observed, confirming the initial idea of Q-balancing.

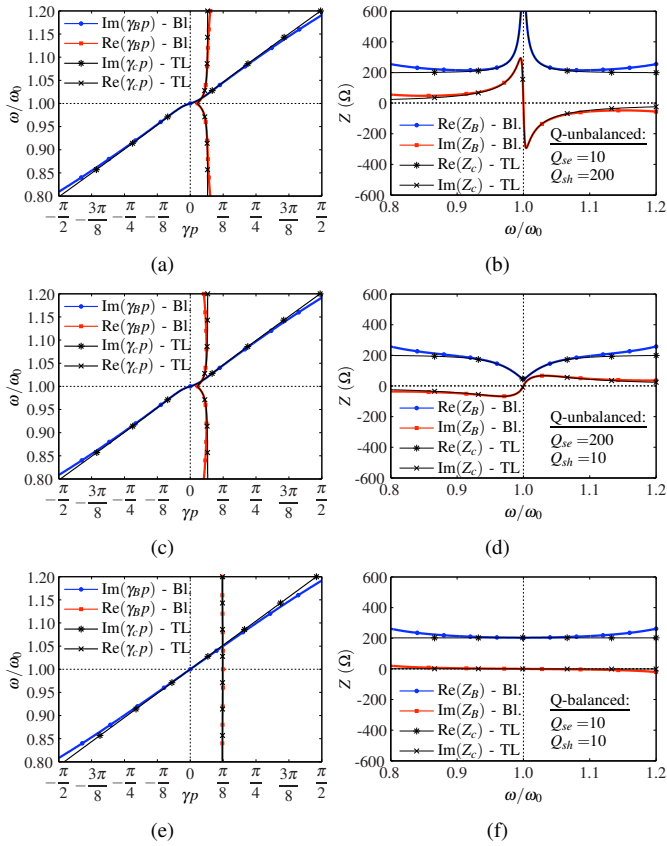


Fig. 2. Comparison of the Bloch model [Eq. (1)] and the TL model [Eq. (2)] for three different Q-conditions. (a) propagation constant and (b) impedance for $Q_{se} < Q_{sh}$. (c) propagation constant and (d) impedance for $Q_{se} > Q_{sh}$. (e) propagation constant and (f) impedance for $Q_{se} = Q_{sh}$.

III. Q-BALANCING CONCEPTS IN SFWA ANTENNAS

The following two concepts, the resistive loading concept and the asymmetry concept, consist in increasing G_{center} so to meet Eq. (7). In all forthcoming EM computations of the quality factors and Bloch impedances, we evaluate a cascade of 10 unit cells using a driven mode analysis so to sufficiently take into account mutual coupling effects as discussed in [7].

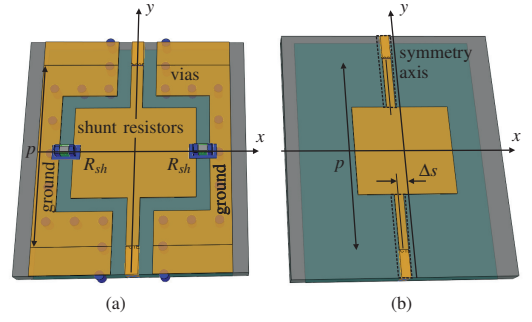


Fig. 3. Concepts for achieving Q-balancing in SFWA LWAs. (a) resistive loading concept, where Q_{sh} is lowered by adding a concentrated element resistor R_{sh} in parallel to G_{center} . (b) asymmetry concept, where an asymmetry with respect to the y -axis is introduced to support broadside shunt radiation and hence lower the Q_{sh} . (The substrate height is $500 \mu\text{m}$ with a permittivity of $\epsilon_r = 3.66$. A cascade of 10 unit cells is evaluated using the FDTD simulator EMPIRE Xccel to take into account mutual coupling effects for accurately extracting the parameters of an infinite periodic structure.)

A. The Resistive Loading Concept

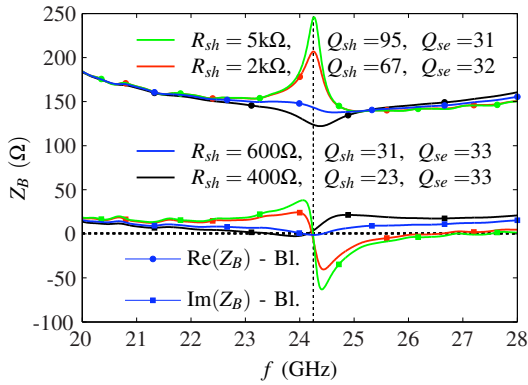
Fig. 3(a) shows the resistive loading concept, where two chip resistors, connected to the ground, are placed at the center of the patch element. Based on the equivalent circuit in Fig. 1(b), it is obvious that these resistors are increasing the shunt conductance G_{center} , since they form a parallel connection. By reducing the resistance R_{sh} , the Q_{sh} is reduced and the condition of Q-balancing is achieved for $R_{sh} = 600 \Omega$ as shown in Fig. 4(a).

B. The Asymmetry Concept

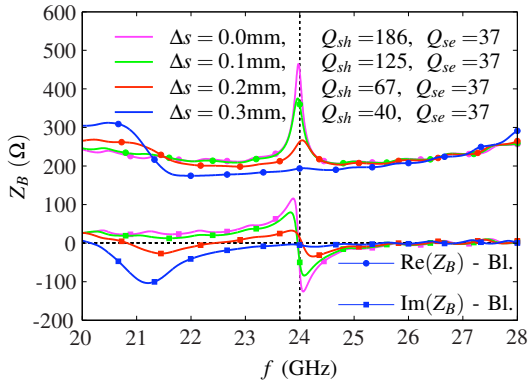
In the asymmetry concept we shift the high impedance TL away from the symmetry line of the patch element, Fig. 3(b). The electric far field component in x -direction of the shunt mode is not canceling anymore for broadside radiation. Therefore, it is possible to tune this amount of orthogonally polarized radiated power by the degree of asymmetry introduced in the antenna cell. Fig. 4(b) shows that an offset $\Delta s = 0.3 \text{ mm}$ is optimum for achieving Q-balancing. In this optimized design, the real and imaginary part of the Bloch impedance show a deviation from the smooth impedance behavior for off-broadside frequencies around 21 GHz. The reason here might be the excitation of transverse modes (x -direction), which is stronger when the degree of asymmetry in the structure is increased. Nevertheless, a constant impedance through broadside has been achieved and confirmed.

C. Radiation Efficiency Improvement using Asymmetry

The resistive loading is degrading the antenna efficiency due to the additional dissipation loss. In this case we still benefit from frequency independent antenna parameters and a constant matching level, but a radiation efficiency improvement is not expected here. For the efficiency evaluation, we therefore focus on the asymmetry concept, where the shunt radiation power is increased. The radiation efficiency turns out to be a better criteria in comparing the performance of such LWA designs, since the gain strongly depends on the LWA's effective length



(a)



(b)

Fig. 4. Q-Balancing results for the SFP LWAs showing the Bloch impedance for comparison. (a) resistive loading concept, where Q-balancing has been achieved with $R_{sh} = 600 \Omega$. (b) asymmetry concept, where Q-balancing has been achieved by shifting the high impedance TL with $\Delta s = 0.3$ mm away from the symmetry line of the patch.

of the radiating aperture. For example, for the symmetric antenna, Q-unbalanced with $\Delta s = 0$ mm, the leakage factor is decreased at broadside (corresponds to Fig. 2(a)) resulting in a larger effective aperture length and hence in an increased gain, which might even overcompensate a gain loss due to efficiency reasons. In order to avoid the separation of these effects, we simply use the radiation efficiency as an integral measure for the LWA performance.

In Fig. 5 the radiation efficiencies, $\eta_{tot} = P_{rad}/P_{incident}$ and $\eta_{ant} = P_{rad}/P_{accepted}$ for the symmetric: $\Delta s = 0$ mm design and optimum: $\Delta s = 0.3$ mm design are compared based on a reference impedance of $Z_0 = 200 \Omega$. These results have been obtained through a drivenmode FDTD analysis using EMPIRE XCcel, where we numerically computed the radiation efficiencies for the LWAs, each composed of 20 unit cells. The efficiency improvement as well as the constant matching level ($\eta_{ant} \approx \eta_{tot}$) as a result of the Q-balancing is clearly confirmed in Fig. 5.

IV. CONCLUSION

In this paper the Q-balancing concept has been illustrated and two methods for achieving Q-balanced designs in LWAs have been proposed. Q-balancing is particularly important,

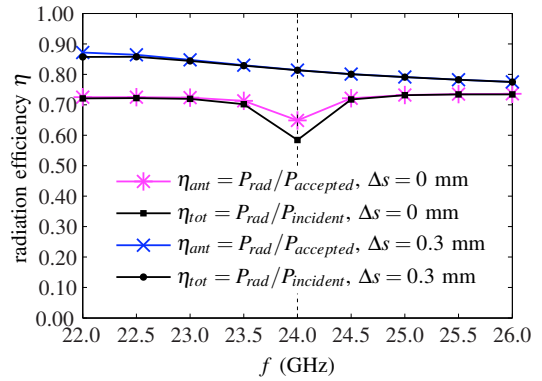


Fig. 5. Radiation efficiencies for Q-unbalanced and Q-balanced designs of Fig. 3(b). Both SFWA LWAs with $\Delta s = 0$ mm and $\Delta s = 0.3$ mm have been setup with 20 unit cells in EMPIRE XCcel (FDTD).

since the wave propagation in a periodic LWA at the broadside frequency is dominated by *resistive* contributions with R and G , rather than *reactive* contributions with L and C . Q-balancing matches the resistive to the reactive part and hence results in frequency independent leakage factor and Bloch impedance for beam scans through broadside.

Using the specific example of the SFWA LWA, we have demonstrated that the two aforementioned methods, the resistive loading and the asymmetry approach can be systematically applied to match the shunt quality factor to the series quality factor. While the resistive loading concept does not provide any efficiency improvement, the Q-balanced asymmetrical LWA shows an increased and constant radiation efficiency level when the radiation beam is scanned through the broadside direction.

REFERENCES

- [1] J. Volakis, *Antenna Engineering Handbook*, 4th ed. McGraw-Hill Professional, June 7 2007.
- [2] D. R. Jackson and A. A. Oliner, *Modern Antenna Handbook*, C. A. Balanis, Ed. Ed. Wiley-Interscience, 2008.
- [3] C. Caloz and T. Itoh, *Electromagnetic Metamaterials: Transmission Line Theory and Microwave Applications*. Wiley-IEEE Press, 2005.
- [4] C. Caloz, T. Itoh, and A. Rennings, "CRLH metamaterial leaky-wave and resonant antennas," *IEEE Antennas Propagat. Mag.*, vol. 50, no. 5, pp. 25–39, Oct. 2008.
- [5] S. Paulotto, P. Baccarelli, F. Frezza, and D. R. Jackson, "Full-wave modal dispersion analysis and broadside optimization for a class of microstrip CRLH leaky-wave antennas," *IEEE Trans. Microwave Theory Tech.*, vol. 56, no. 12, pp. 2826–2837, December 2008.
- [6] J. S. Gomez-Diaz, D. Cañete Rebenaque, and A. Alvarez-Melcon, "A simple CRLH LWA circuit condition for constant radiation rate," *IEEE Antennas Wireless Propagat. Lett.*, vol. 10, pp. 29–32, 2011.
- [7] S. Otto, A. Rennings, K. Solbach, and C. Caloz, "Transmission line modeling and asymptotic formulas for periodic leaky-wave antennas scanning through broadside," *IEEE Trans. Antennas Propagat.*, vol. 59, no. 10, October 2011.
- [8] D. M. Pozar, *Microwave Engineering*. J. Wiley & Sons, New York, 3rd ed., 2004.
- [9] S. Otto, A. Rennings, T. Liebig, C. Caloz, and K. Solbach, "An energy-based circuit parameter extraction method for CRLH leaky-wave antennas," in *4rd European Conference on Antennas and Propagation*, Barcelona, Spain, April 2010.